

Supplementary Information

Bacterial homoserine lactones as nanocomposite fertilizer and defense regulator for chickpeas

Govind Sharan Gupta^{a, #}, Arun Kumar^{b, #} and Nishith Verma^{a, b*}

^aCenter for Environmental Science and Engineering, Indian Institute of Technology Kanpur, Kanpur 208016, India.

^bDepartment of Chemical Engineering, Indian Institute of Technology Kanpur, Kanpur 208016, India.

*Corresponding author. Tel.: +91 512 259 7704; fax: +91 512 259 0104. E-mail address: vermanishith@gmail.com (N. Verma).

Govind Sharan Gupta and Arun Kumar contributed equally to this work.

1.1. Synthesis of Fe-CNF

As-received ACFs were pre-treated with 1 L 0.05 M HNO_3 at 80 °C for 2 h, washed with MQ water to neutralize the surface, and then vacuum-dried at 200 °C for 12 h. This step removed impurities from the surface of the ACF. The pre-treated ACF sample (2 g) was stirred in 200 ml 0.4 M $\text{Fe}(\text{NO}_3)_3 \cdot 9\text{H}_2\text{O}$ solution for 2 h, and SDS was used as a surfactant in the salt solution to prevent agglomeration. The salt-impregnated ACF was air-dried at room temperature (~30 °C) for 8 h and then vacuum-dried at 200 °C for 12 h. Calcination of the salt-impregnated ACF sample was performed at 400 °C for 4 h under a N_2 gas flow (200 standard cubic cm per min (sccm)) followed by hydrogen reduction at 500 °C for 2 h (gas flow rate = 150 sccm). These steps resulted in the conversion of Fe nitrate into Fe oxides and then into elemental or zero valent Fe as NPs. The CNFs were grown over Fe-ACF using catalytic chemical vapor deposition (CVD) of acetylene (flow rate = 30 sccm) for 0.5 h. The Fe NPs dispersed in ACF served as the CVD catalyst. The CNF-grown sample is hereafter referred as Fe-CNF/ACF. The Fe-CNF/ACF were ball-milled for 15 min to detach the Fe-CNF from the ACF substrate and then dispersed in water. The powdered Fe-CNFs were isolated from the dispersion by magnetic separation and then allowed to interact with AHL. A detailed explanation on the interaction of AHL and Fe-CNF has been provided in the manuscript.

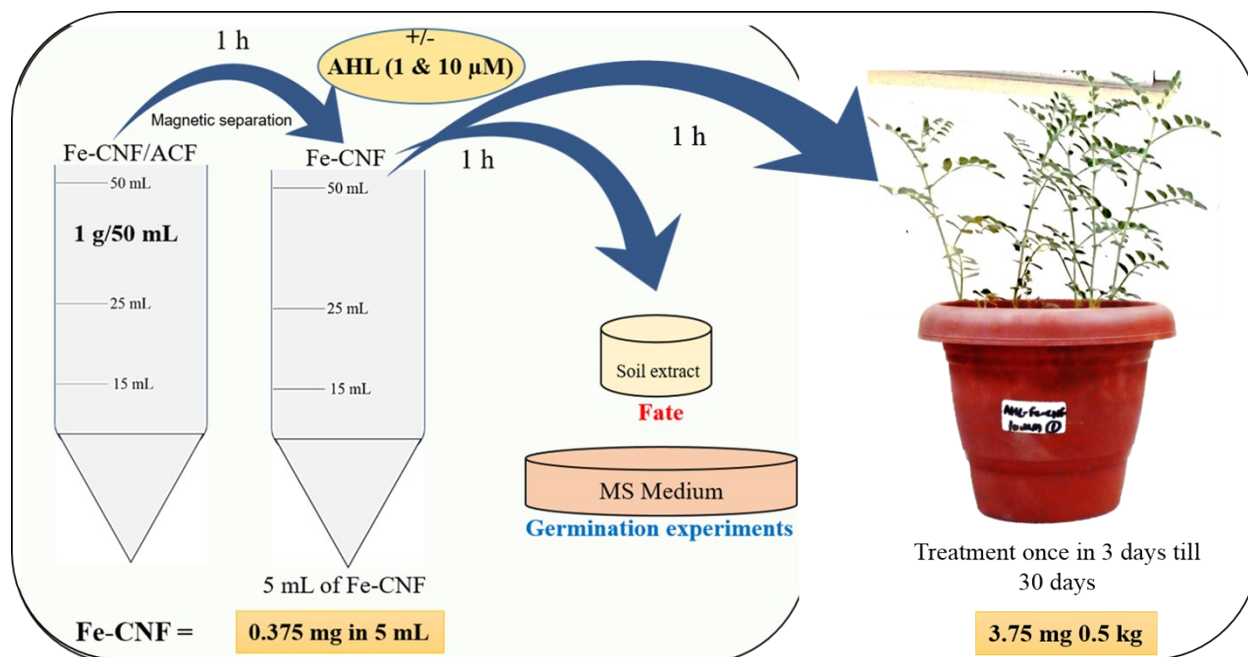


Fig. S1. AHL/Fe-CNF isolation and treatment procedure for fate, germination experiments and plant irrigation.

1.2. Characterization of Fe-CNF and AHL/Fe-CNF NCs

Scanning electron microscopy coupled with energy dispersive X-ray spectroscopy (SEM-EDS):

Surface morphology of the ACF substrate and Fe-CNF samples was examined using a field emission scanning electron microscope (FE-SEM; Supra 40 VP, Zeiss, Germany) at an accelerating voltage of 15 kV. A liquid suspension of Fe-CNF was prepared by the drop coating method.¹ The images were captured without sputter coating.

X-ray diffraction spectroscopy (XRD): The phase analysis spectrum of Fe-CNF was recorded by powder XRD with an X'Pert X-ray diffractometer (PANalytical BV, Almelo, The Netherlands) at 40 kV and 200 mA with Cu K α radiation ($\lambda = 1.5418 \text{ \AA}$).

Texture analysis by Brunauer–Emmett–Teller (BET) method: The BET analysis was performed as described elsewhere.² Surface area and total pore volume of Fe-CNF was determined at

liquid N₂ temperature (77 K) using an Autosorb-1C instrument (Quantachrome, Boynton Beach, FL, USA). The samples were degassed at 150 °C for 12 h before analysis. A relative pressure (P/P₀) of < 0.15 was selected to calculate the BET surface area because of the predominantly microporous characteristics of the materials and linearity of the isotherm over the selected pressure range. Total pore volume of the samples was calculated at the relative pressure of 0.9999.

1.3. Interaction of AHL with Fe-CNF

The composite solution of AHL/Fe-CNF was analyzed after 1 h of interactions, using Zeta-sizer, zeta potential, FTIR and GC-FID. The individual solutions of AHL and Fe-CNF were also analyzed simultaneously, where required.

Hydrodynamic size of Fe-CNF and AHL/Fe-CNF NCs: Average hydrodynamic sizes of Fe-CNF and AHL/Fe-CNF were determined by the dynamic light scattering (DLS) technique using a Zeta-sizer Nano-ZS instrument equipped with a 4.0-mW, 633-nm laser (Model ZEN3600; Malvern Instruments, Malvern, UK).

Electro-kinetic changes in Fe-CNF and AHL/Fe-CNF NCs: Electro-kinetic measurements including zeta potential (ζ -potential) were taken for Fe-CNF alone and a suspension of Fe-CNF with AHL, using the Zeta-sizer Nano-ZS instrument.

Fourier-transform infrared (FTIR) spectroscopy: The ligand interaction between AHL and Fe-CNF was determined using attenuated total reflectance (ATR) and Fourier-transform infrared (FT-IR) (Bruker Tensor 27 spectrophotometer, Germany) spectroscopy. The samples were scanned over the wavelength range of 500–4000 cm⁻¹. MilliQ water was used as a background

to ensure its negligible interference on the spectra of AHL and Fe-CNF. The FTIR measurements were taken three times and the average was presented to ensure reproducibility.

Gas chromatography- flame ionization detector (GC-FID): Loading efficiency of AHL in Fe-CNF was determined using GC-FID. The AHLs from the aqueous solution of AHL/Fe-CNF NC were extracted using n-heptane. The samples were analysed using a gas chromatography (model 5700, Nucon Eng. Co., India) equipped with the HP-5MS column (30 m long x 0.250 mm i.d.) and a flame ionization detector (FID). The method is described by Sheng et. al.³ Nitrogen was used as the carrier gas. Hydrogen was used as the flame source in FID. The gaseous streams were passed through silica gel to remove moisture from the gasses. The GC inlet temperature was set at 290 °C. Oven temperature was ramped from 100 to 150 °C at a rate of 35 °C per min and then increased by 15 °C per min to 280 °C before being held at 280 °C for 6 min. Prior to the measurements, calibration was performed using a range of known concentrations of AHL to correlate the GC signals with the concentrations. The calibration data were linearly fitted using Origin. The R^2 value is found to be 0.99774 which shows that the experimental data are close to the regression line. Three replicates of each samples were used to observe the corresponding area under the peaks. Quality of data was ensured by taking average of all three values. Typical calibration curve for AHL concentration using GC-FID is presented in Fig. S2.

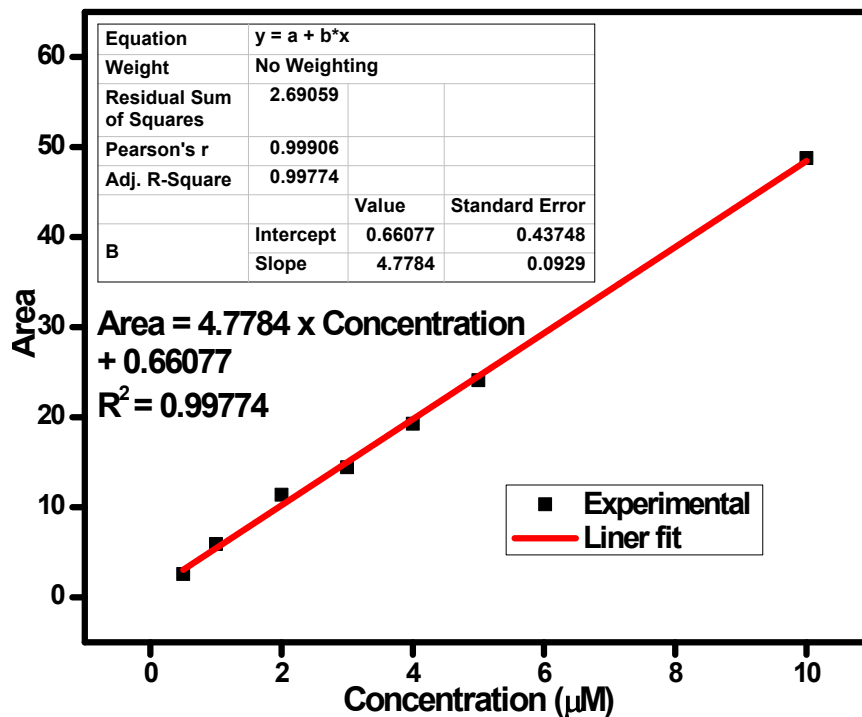
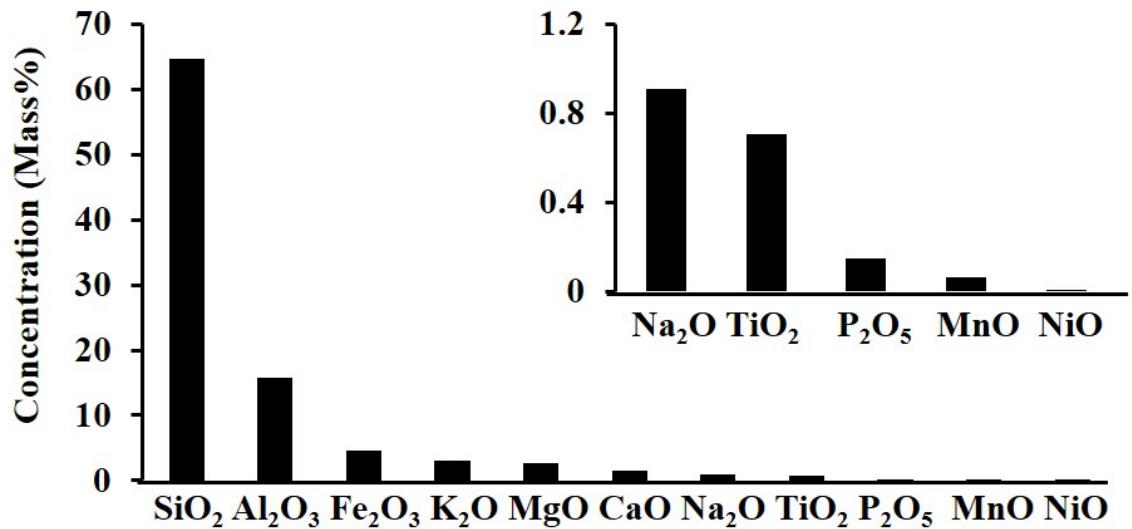


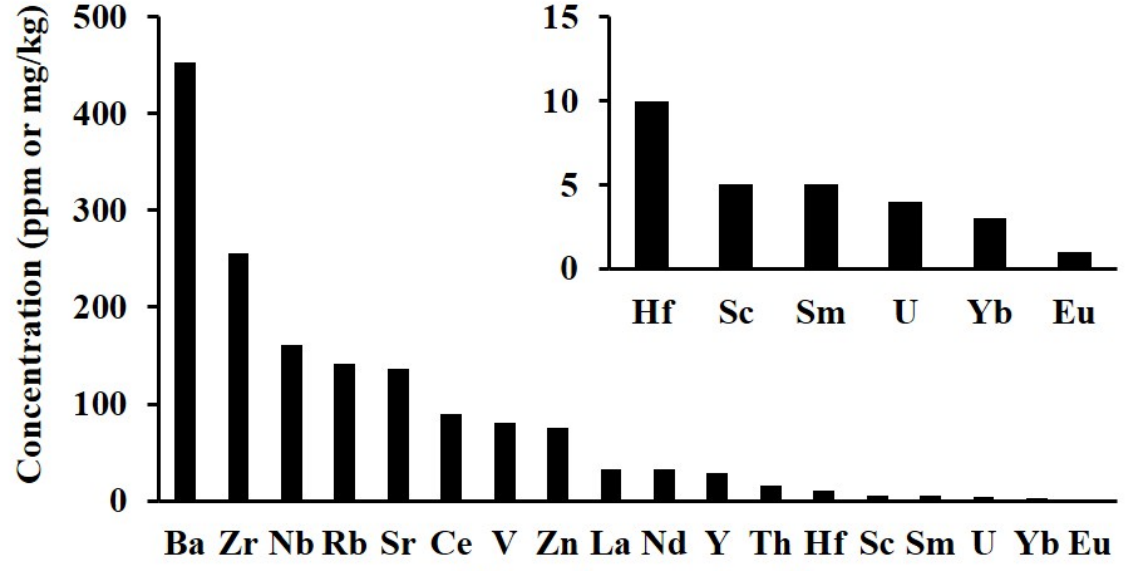
Fig. S2. GC calibration for AHL using FID signals

1.4. Characterization of the soil

Sandy-clay agricultural soil was collected from the campus of Indian Institute of Technology Kanpur, central India. The soil sample was sieved (mesh size 4 mm) to remove stones, roots, and litter before use in the laboratory. The sample was characterized for pH and elemental content. Total elemental contents of the soil, including macro- and micro-nutrients were determined using x-ray fluorescence spectroscopy (WD-XRF, Rigaku, Japan). The pH of the soil solution was measured to be 7.56 ± 0.04 . Fig. S3 presents the elemental analysis data of the soil.



Major elements in soil



Trace elements in soil

Fig. S3. XRF analysis of soils used in the plant experiments.

1.5. Experimental design on nanocomposites exposure

Table S1: Experimental design for the germination experiments (columns and rows describe the different stress and treatment groups, respectively)

Stress group →	(1) Control (No stress)	(2) Oxidative stress	(3) Salinity stress
Treatment group ↓			
(1) Control	–	H ₂ O ₂ (5 mM)	NaCl (200 mM)
(2) Fe-CNF	Fe-CNF (75 µg/mL)	Fe-CNF (75 µg/mL) + H ₂ O ₂ (5 mM)	Fe-CNF (75 µg/mL) + NaCl (200 mM)
(3) AHL	AHL (10 µM)	AHL (10 µM) + H ₂ O ₂ (5 mM)	AHL (10 µM) + NaCl (200 mM)
(4) AHL(1 µM)/Fe-CNF	AHL (1 µM)/Fe-CNF (75 µg/mL)	AHL (1 µM) + Fe-CNF (75 µg/mL) + H ₂ O ₂ (5 mM)	AHL (1 µM) + Fe-CNF (75 µg/mL) + NaCl (200 mM)
(5) AHL(10 µM)/Fe-CNF	AHL (10 µM)/Fe-CNF (75 µg/mL)	AHL (10 µM) + Fe-CNF (75 µg/mL) + H ₂ O ₂ (5 mM)	AHL (10 µM) + Fe-CNF (75 µg/mL) + NaCl (200 mM)

Table S2: Experimental design for plant growth experiments (column 2 and 3 depicts the different stress groups and rows depicts the different treatment groups).

Plant group →	(1) Control (No stress)	(2) Fungal stress
Treatment group ↓		
(1) Control	–	Fungal infection
(2) Fe-CNF	Fe-CNF (75 µg/mL)	Fe-CNF (75 µg/mL) + Fungal infection
(3) AHL	AHL (10 µM)	AHL (10 µM) + Fungal infection
(4) AHL(1 µM)/Fe-CNF	AHL (1 µM)/Fe-CNF (75 µg/mL)	AHL (1 µM) + Fe-CNF (75 µg/mL) + Fungal infection
(5) AHL(10 µM)/Fe-CNF	AHL (10 µM)/Fe-CNF (75 µg/mL)	AHL (10 µM) + Fe-CNF (75 µg/mL) + Fungal infection

1.6. Assessment techniques and assay for the translocation and distribution of AHL/Fe-CNF within the plants

Translocation and distribution of Fe-CNF and AHL/Fe-CNF NCs within the plants were determined by microscopic observation, elemental analysis, and mapping using a field emission scanning electron microscope (SEM; Supra 40 VP, Zeiss, Oberkochen, Germany) in combination with energy-dispersive x-ray spectroscopy (EDS).

Optical microscopy: Thin sections of the root and shoot were prepared by hand using sharp blades. The sections were placed on glass slides in ibidi mounting medium to protect them from drying and shrinking. All images were captured under an optical microscope (Leica Microsystems, Buffalo Grove, IL, USA) at 4× magnification. The experiment was repeated at least twice at the same conditions and more than ten images were captured from each sample.

SEM-EDS analysis: Samples of plant shoots were prepared for the SEM-EDS analysis by prefixation of the thin sections with 5% glutaraldehyde for 20 min in 1× phosphate buffer saline (PBS). The samples were washed three times with PBS and then dehydrated in an ethanol gradient series (15%, 30%, 50%, 70%, and 100%) for 20 min at each concentration. The samples were dried overnight at room temperature on the SEM stubs. At least five images were captured from different regions in each sample.

Atomic absorption spectroscopy (AAS): Concentrations of Fe in the germinated radicle, root, shoot, and leaf of the control and treated plants were determined using flame atomic absorption spectroscopy (AAS; Varian AA-240, Palo Alto, CA, USA). Approximately 1 g of the dried samples of the leaf, root, and shoot were weighed in sterile glass test tubes, and then slowly digested in heated sand with concentrated HNO₃ (70%). The samples were digested until the solution became clear. Final volume was adjusted to 5 ml with 1% HNO₃. The Fe concentration was measured using AAS with an acetylene flame.⁴ Before analysis, the AAS instrument was calibrated using the standard Fe solution of known concentration (Fig.S4). Three replicates of reading were recorded for a high accuracy. Moreover, all samples were prepared in triplicate. The presented data are mean ± SD of three experiments.

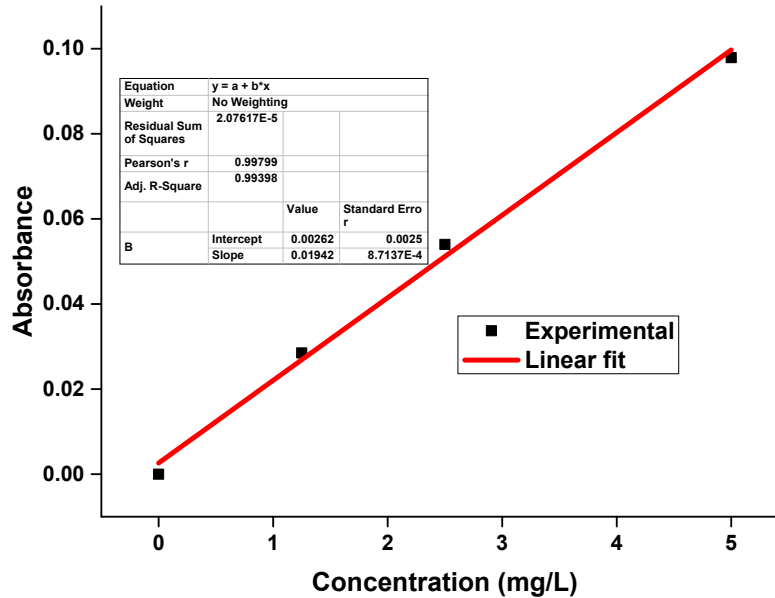


Fig. S4. Calibration of AAS instrument using standardized Fe solution

Measurement of chlorophyll contents in the leaf:

Chlorophyll (Chl) was extracted from the leaves as per the protocol used by Ashfaq et al.⁵ Briefly, approximately 100 mg leaf tissues were selected from each freshly harvested plant and ground in liquid nitrogen. Approximately 10 mL of 80% acetone was added to form a paste. The mixture was incubated overnight at 4 °C, then centrifuged at 717 RCF for 15 min. Absorbance of the supernatant was measured at 645 and 663 nm wavelengths using ultraviolet–visible (UV–Vis) spectrophotometer (Varian Cary 100, Darmstadt, Germany). Acetone (80%) was run as blank to measure the chlorophyll absorbance. The Chl-a, Chl-b and total Chl contents ($\mu\text{g mL}^{-1}$) were determined using the formulas:

$$\text{Chl-a} = 11.24 \times A_{663} - 2.04 \times A_{645}$$

$$\text{Chl-b} = 20.13 \times A_{645} - 4.19 \times A_{663}$$

$$\text{Total Chl} = \text{Chl-a} + \text{Chl-b}$$

Measurement of protein contents in the shoot:

Protein contents in the shoots of control and treated plants were determined in accordance with the method described by Ashfaq et al.⁵ Briefly, 500 mg of shoot tissue were ground in liquid nitrogen and then mixed with 5 mL of 1× PBS buffer. The mixture was incubated at room temperature in dark for 1 h. The sample was centrifuged at 717 RCF for 30 min. Next, 5 mL of alkaline-copper solution was mixed into 1 mL of the supernatant. Approximately 0.5 mL Folin’s reagent was mixed into the supernatant–alkaline solution mixture and incubated for 30 min in

dark at room temperature. Protein concentration in the mixture was measured at 660 nm wavelength, using the UV–Vis spectrophotometer.

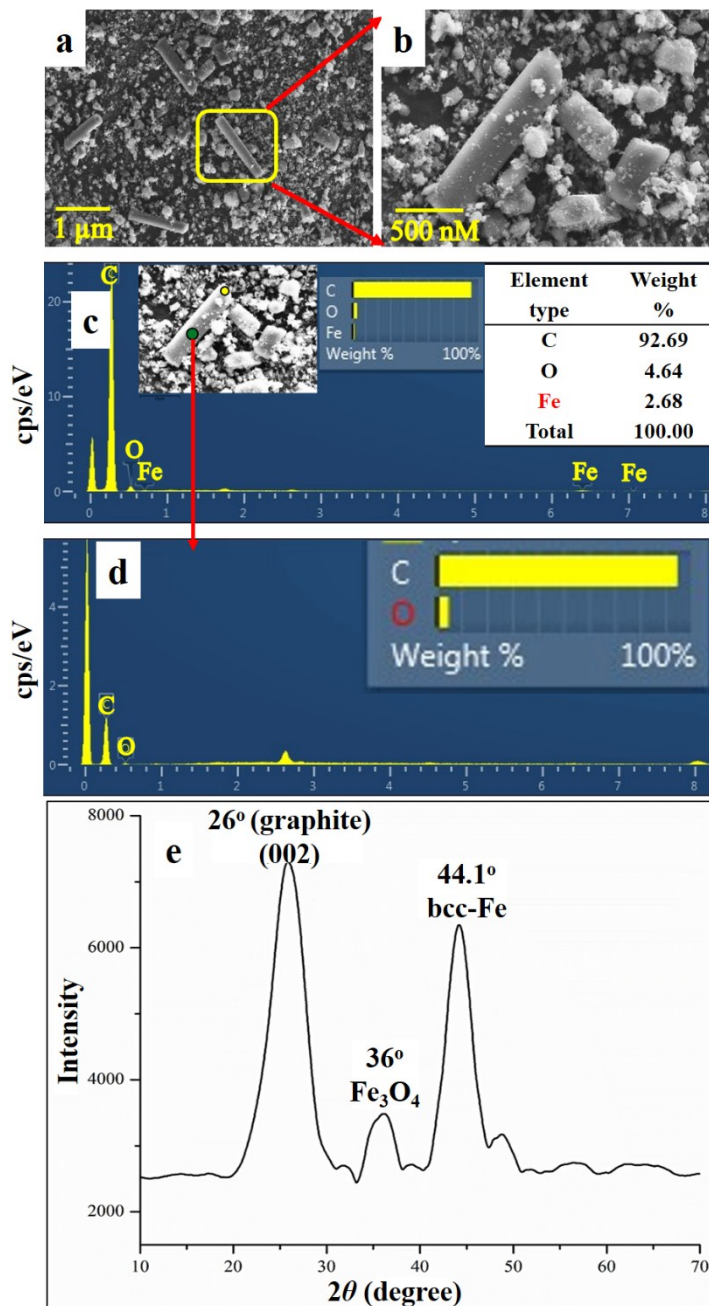


Fig. S5. (a-b) Low- and high-magnification scanning electron micrographs of separated Fe-CNF. (c-d) Area and point energy dispersive X-ray spectra of separated Fe-CNF. (e) X-ray diffraction spectrum of Fe-CNF.

Table S3: Iron loading in the ACF, Fe-CNF/ACF and Fe-CNF.

Sample Name	Fe (mg/g)
ACF	0 ± 0
Fe-CNF/ACF	6.2 ± 0.9
Fe-CNF	3.7 ± 0.1

Data presented are mean ± SD of three experiments.

Table S4: Polydispersity index (PDI) of NCs in the soil extract.

Samples	0 h	24 h	48 h
SE	0.27 ± 0.0	0.32 ± 0.1	0.37 ± 0.1
SE_AHL	0.28 ± 0.0	0.47 ± 0.0	0.49 ± 0.1
SE_Fe-CNF	0.70 ± 0.1	0.49 ± 0.1	0.72 ± 0.2
SE_AHL (1 μM)/Fe-CNF	0.68 ± 0.1	0.41 ± 0.0	0.66 ± 0.1
SE_AHL (10 μM)/Fe-CNF	0.61 ± 0.2	0.49 ± 0.1	0.73 ± 0.1

Data presented are mean ± SD of three experiments.

Table S5: AHL Adsorption and loading efficiency of Fe-CNF after 1 h of interaction (AHL concentration were determined using GC-FID).

Initial AHL concentration (μM)	Equilibrium AHL conc. (μM)	% Loading efficiency
1	0.5 ± 0.01	54 ± 1.9
10	5.60 ± 0.2	44 ± 2.4

Data presented are mean \pm SD of three experiments.

1.7. Correlation for the AHL surface coverage on Fe-CNF

ρ = bulk density of AHL (g/cc)

M = molecular weight (g/mol)

$$V, \text{ molar volume} = \frac{\rho}{M} \text{ (cc/mol)}$$

Assuming that intermolecular space between the AHL molecules is negligible,

$$V_{\text{molecule}}, \text{ molecular volume} = \frac{V}{N_A} \text{ (cc/molecule); where } N_A = \text{Avogadro's number.}$$

Assuming a spherical molecule of diameter D , the area cover by each molecule is $\frac{\pi D^2}{4}$ and surface covered like a square screen of length, $L = D$

Therefore, a , surface area covered by each molecule that sticks onto the adsorbent site is

$$a = L^2 = \left(\frac{6V_{\text{molecule}}}{\pi} \right)^{2/3} \text{ (cm}^2\text{/molecule)}$$

If C_i = initial concentration of AHL (mol/ml)

total no. (N) of molecules of AHL adsorbed at the adsorbent surface = $C_i \times v \times \eta \times N_A$

where, v (ml) is the volume of AHL aqueous solution used in the adsorption tests and η (%) is the loading efficiency of the AHL on adsorbent.

Therefore, A_{adsorbed} , total area of the adsorbed molecules = $N \times a$

A_{Total} , total surface area of the adsorbent taken for the adsorption experiment = $w \times v \times S_{\text{BET}}$

where, w (g/ml) weight of adsorbent per ml of AHL aqueous solution and S_{BET} (cm^2/g) specific surface area of the adsorbent.

f, the fractional surface coverage = $\frac{A_{\text{adsorbed}}}{A_{\text{Total}}}$

Therefore,

$$\text{or } f = \frac{N \times a}{w \times v \times S_{\text{BET}}} = \frac{C_i \times v \times \eta \times N_A \times a}{w \times v \times S_{\text{BET}}} = \frac{C_i \times \eta \times N_A \times a}{w \times S_{\text{BET}}}$$

For AHL: $\rho = 1.3 \text{ g/cc}$, $M = 187.193 \text{ g/mol}$, $N_A = 6.23 \times 10^{23}$

From the experimental conditions: $C_i = 1 \mu\text{M} = 10^{-9} \text{ (mol/ml)}$, $v = 50 \text{ ml}$, $\eta = 54 \%$, $w = 75 \mu\text{g/ml} = 75 \times 10^{-6} \text{ g/ml}$, $S_{\text{BET}} = 67 \text{ m}^2/\text{g} = 67 \times 10^4 \text{ cm}^2/\text{g}$

Substituting the known values, $f = 0.0387$ i.e. % surface coverage is calculated to be 3.87 which is based on the BET surface area of the Fe-CNF.

Based on the various properties of AHL and Fe-CNF a correlation for the surface coverage area was developed and presented in the supplementary information. The correlation estimates an approximately 4% surface coverage of Fe-CNF within 1 h of interaction. A low surface area coverage of AHL molecules onto the Fe-CNF surface can be explained based on three major scenarios: (1) possibility of a monolayer coverage of AHL, (2) a high BET surface area of Fe-CNF, which considers multilayer surface coverage, and (3) the assumption that intermolecular spacing between the molecules is negligible.

1.8. Fe content in germinated seedlings

Experiments to determine the Fe contents in the emerging seedlings were performed. Trace of Fe was found in the range of 0.05 to 0.08 mg/g of dry weight of the seedlings in the control as well as in the AHL treated seedlings. Similar quantities of trace Fe in raw chickpea seeds were reported elsewhere⁶. However, Fe contents in the Fe-CNF- and Fe-CNF/AHL-treated seedlings were found to be in the range of 0.07 to 0.18 mg/g, which confirms at least 100% higher Fe uptake in the Fe-CNF- or Fe-CNF/AHL-treated seeds. A reduced Fe uptake capacity was measured in the stressed seedlings, attributed to the competitive translocation of stressing compounds with Fe-CNF within the seedling cells.

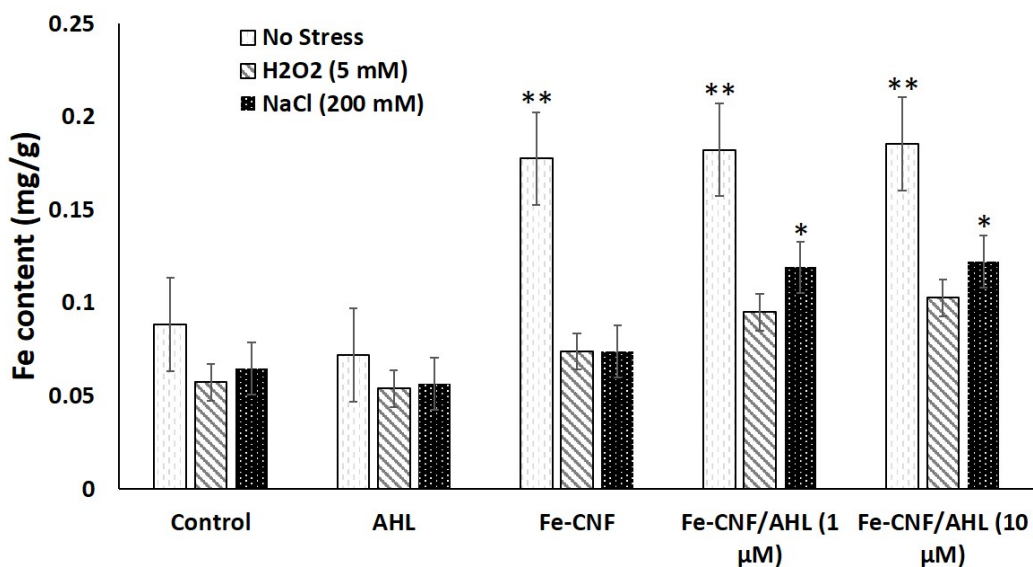


Fig. S6. Distribution of Fe in the germinated seedlings post-exposure to Fe-CNF and AHL/Fe-CNF NCs. Data are the mean \pm SD of three experiments. Significance was determined using one-way ANOVA with Dunnett's post-hoc test. * $p < 0.05$; ** $p < 0.001$.

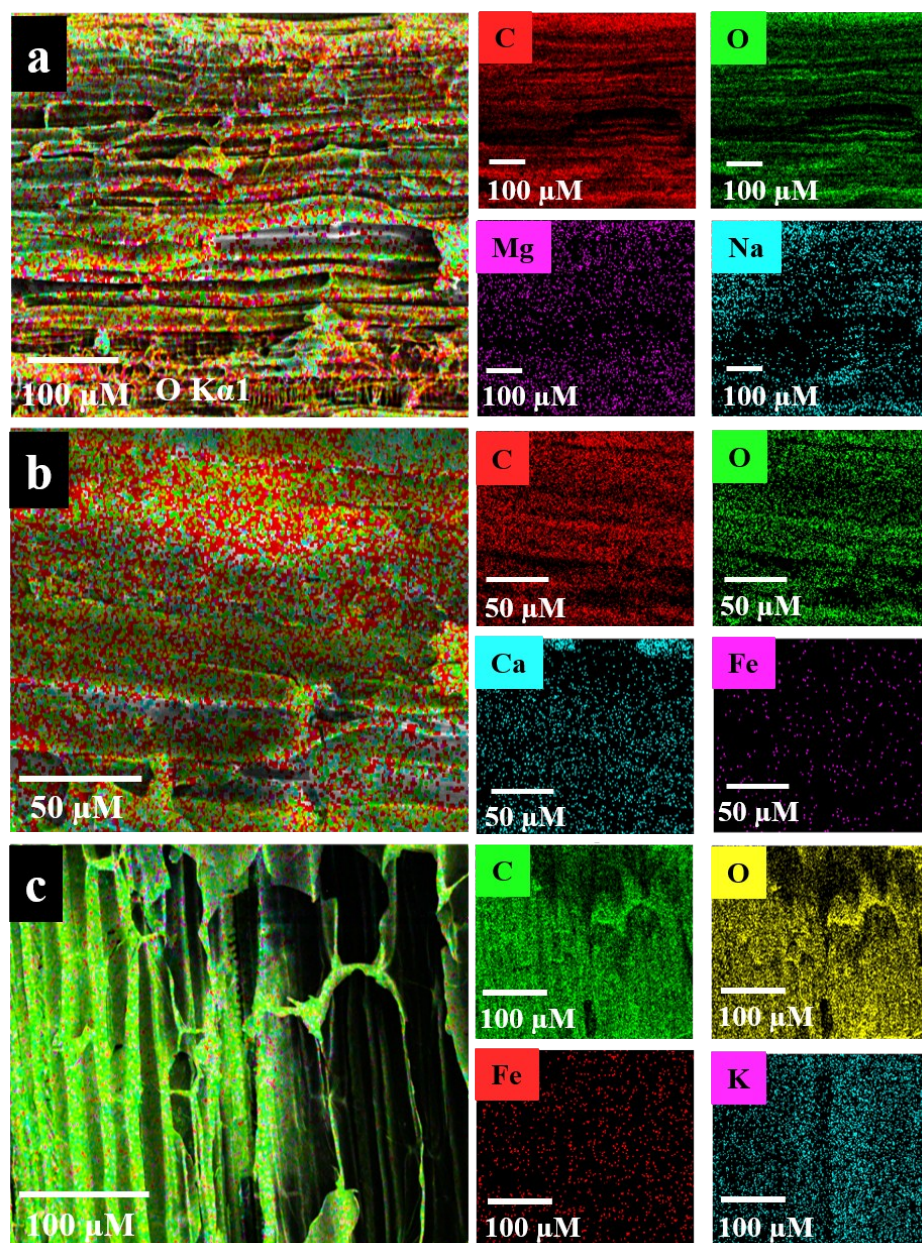


Fig. S7. EDS mapping of plants for the distribution of Fe-CNF. (a) control, (b) Fe-CNF and (c) AHL (10 μM)/Fe-CNF NC.

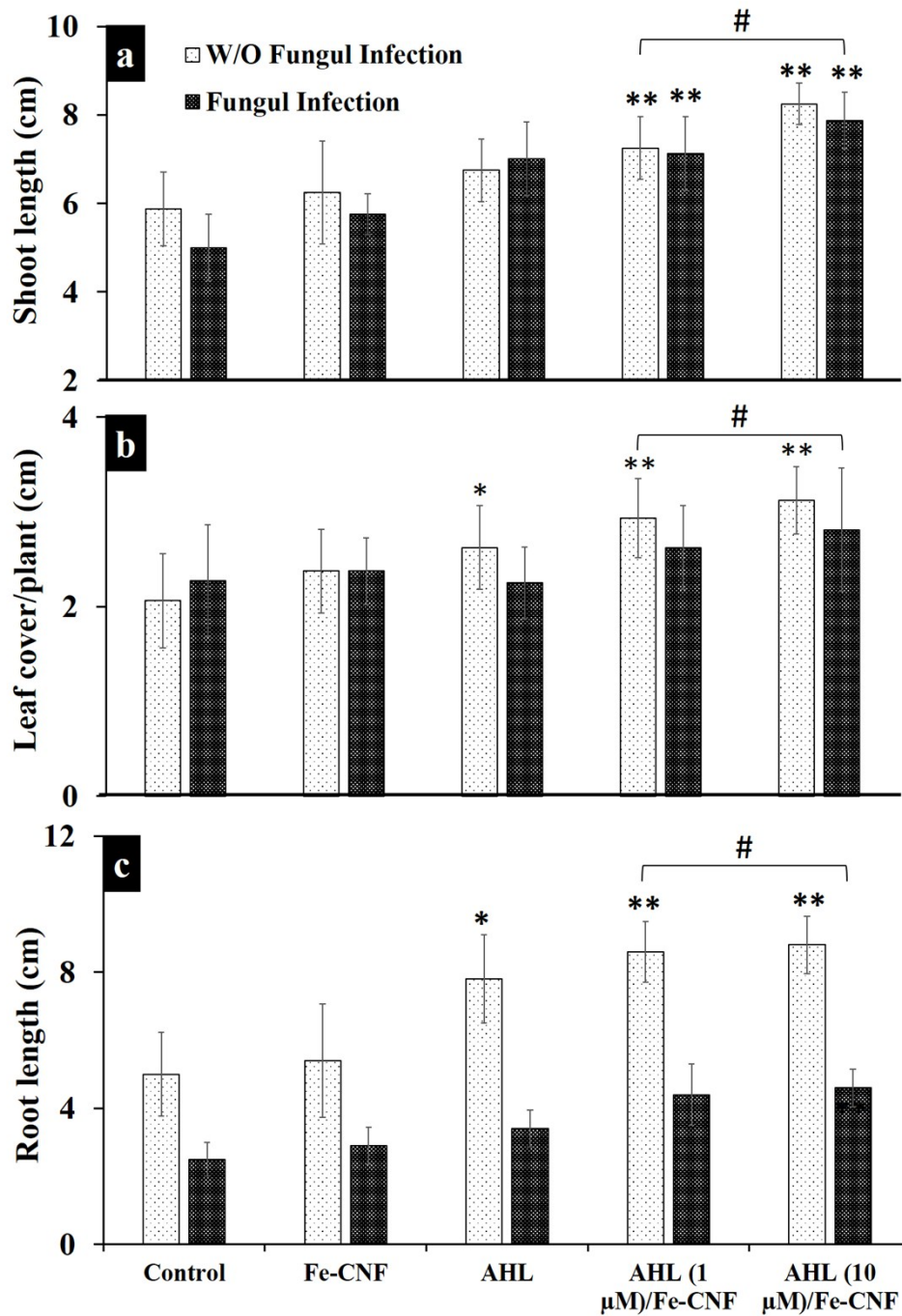


Fig. S8. Shoot and root lengths, and leaf cover in chickpea plants post-exposure to NCs with or without fungal infection. (a) Shoot length, (b) leaf cover, and (c) root length. (Increase of each length with NCs application). The significance value was calculated using the one-way ANOVA (ordinary) with Tukey's post hoc test. * $p < 0.05$, ** $p < 0.001$, statistically significant with respect to control; #statistically significant with respect to the Fe-CNF treatment. $p > 0.05$ between the NCs treatments.

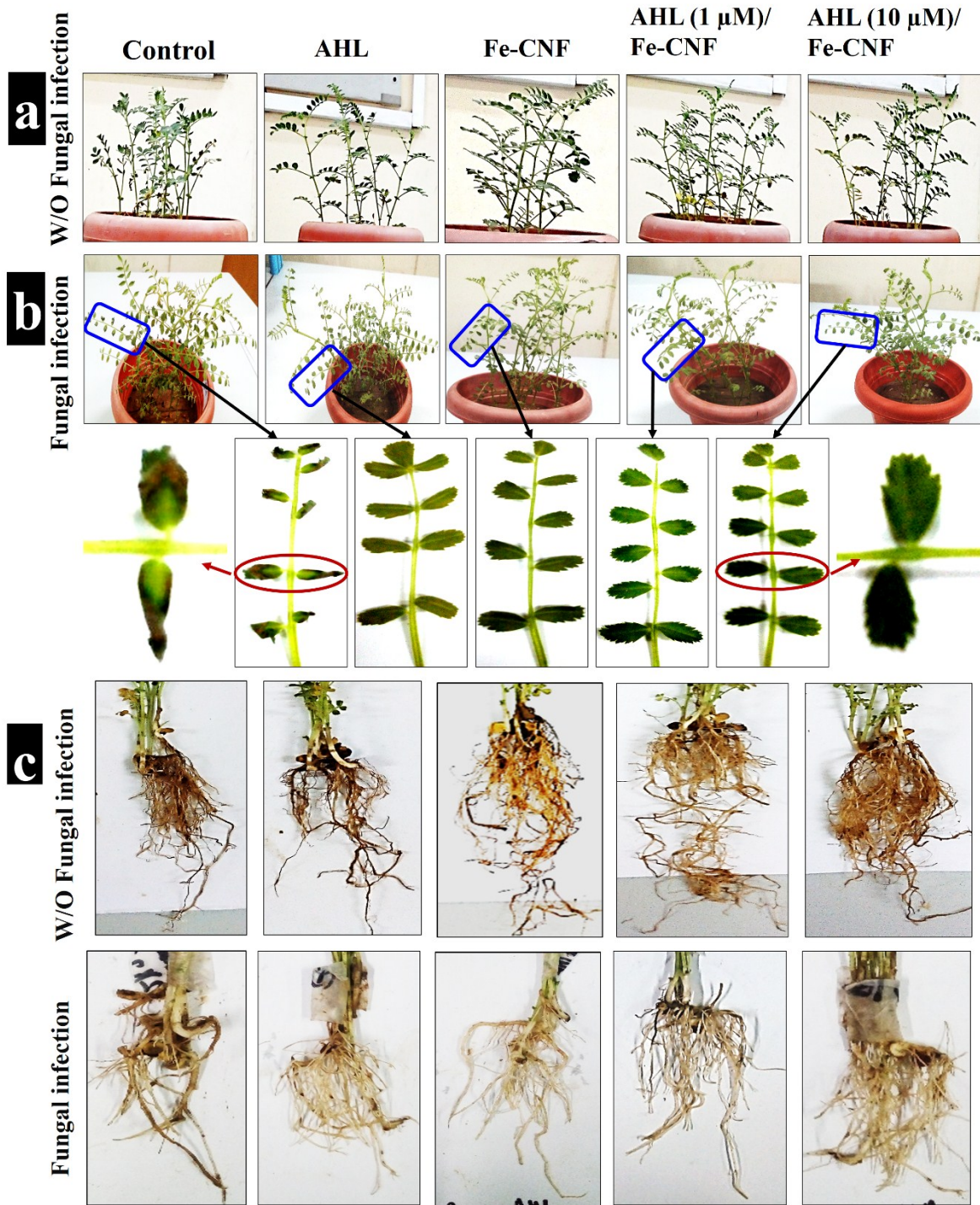


Fig. S9. Micrographs of chickpea plants grown with or without (W/O) fungal infection in the presence/absence of AHL/Fe-CNF NCs. (a) shoot, (b) leaf, and (c) root system. (Fungal infection causes curling and yellowing of leaves in control plants, which is otherwise absent in the NC treated leaves.)

References:

1. G. S. Gupta, A. Kumar, R. Shanker and A. Dhawan, Assessment of agglomeration, co-sedimentation and trophic transfer of titanium dioxide nanoparticles in a laboratory-scale predator-prey model system, *Sci. Rep.*, 2016, **6**, 31422.
2. Y. N. Prajapati and N. Verma, Fixed bed adsorptive desulfurization of thiophene over Cu/Ni-dispersed carbon nanofiber, *Fuel*, 2018, **216**, 381-389.
3. H. Sheng, F. Wang, C. Gu, R. Stedtfeld, Y. Bian, G. Liu et. al., Sorption characteristics of N-acyl homoserine lactones as signal molecules in natural soils based on the analysis of kinetics and isotherms. *RSC Advances*, 2018, **8**, 9364-9374.
4. R. A. Scott, J. Weil, P. T. Le, P. Williams, R. G. Fray, S. B. von Bodman and M. A. Savka, Long- and short-chain plant-produced bacterial N-acyl-homoserine lactones become components of phyllosphere, rhizosphere, and soil, *MPMI*, 2006, **19**, 227-239.
5. M. Ashfaq, N. Verma and S. Khan, Carbon nanofibers as a micronutrient carrier in plants: efficient translocation and controlled release of Cu nanoparticles, *Environ. Sci.: Nano*, 2017, **4**, 138-148.
6. A.M. Ramírez-Ojeda, R. Moreno-Rojas and F. Cámara-Martos, Mineral and trace element content in legumes (lentils, chickpeas and beans): Bioaccessibility and probabilistic assessment of the dietary intake, *J. Food Compos. Anal.*, 2018, **73**, 17-28.